

# Generalized $\mathbb{Z}_2 \times \mathbb{Z}_2$ in Scaling neutrino Majorana mass matrix and baryogenesis via flavored leptogenesis

Roopam Sinha\*, Rome Samanta † Ambar Ghosal‡

Saha Institute of Nuclear Physics, HBNI, 1/AF Bidhannagar, Kolkata 700064, India

June 25, 2022

## Abstract

We investigate the consequences of a generalized  $\mathbb{Z}_2 \times \mathbb{Z}_2$  symmetry on a scaling neutrino Majorana mass matrix. It enables us to determine definite analytical relations between the mixing angles  $\theta_{12}$  and  $\theta_{13}$ , maximal CP violation for the Dirac type and vanishing for the Majorana type. Beside the other testable predictions on the low energy neutrino parameters such as  $\beta\beta 0\nu$  decay matrix element  $|M_{ee}|$  and the light neutrino masses  $m_{1,2,3}$ , the model also has intriguing consequences from the perspective of leptogenesis. With the assumption that the required CP violation for leptogenesis is created by the decay of lightest ( $N_1$ ) of the heavy Majorana neutrinos, only  $\tau$ -flavored leptogenesis scenario is found to be allowed in this model. For a normal ordering of light neutrino masses,  $\theta_{23}$  is found to be less than its maximal value, for the final baryon asymmetry  $Y_B$  to be in the observed range. Besides, an upper and a lower bound on the mass of  $N_1$  have also been estimated. Effect of the heavier neutrinos  $N_{2,3}$  on final  $Y_B$  has been worked out thereafter. The predictions of this model will be tested in the experiments such as GERDA-II, T2K, NO $\nu$ A, DUNE etc.

---

\*roopam.sinha@saha.ac.in

†rome.samanta@saha.ac.in

‡ambar.ghosal@saha.ac.in

# 1 Introduction

The neutrino oscillation data, adhering to the bound on the sum of the three electroweak neutrino masses and the results of  $\beta\beta_{0\nu}$  decay experiments severely constrain the textures of light neutrino mass matrix. Admissible textures of the mass matrix satisfying the above experimental constraints thus can be tested in future through their predictions regarding the yet unresolved issues such as the hierarchy of neutrino masses, octant determination of  $\theta_{23}$ , and particularly, CP violation in the leptonic sector which might have implication on the matter-antimatter asymmetry of the universe. Besides, if neutrino is a Majorana particle, the prediction of Majorana phases will also serve as an added ingredient to discriminate different models. From the symmetry point of view thus it is a challenging task to integrate theoretical considerations involving different symmetry/ansatz in addition to the Standard Model (SM).

Recently, the idea of residual symmetry [1,2] has attracted much attention to explore the flavor structure of light neutrino mass matrix. In this approach, the neutrino mass matrix is attributed in terms of some residual or remnant symmetry of a horizontal flavor group. It can be shown that Majorana type nondegenerate light neutrinos lead to an invariance of the effective light neutrino mass matrix under a  $\mathbb{Z}_2 \times \mathbb{Z}_2$  symmetry accompanied with a charged lepton mass matrix that enjoys a  $\mathbb{Z}_n$  invariance with  $n > 2$  [1]. Now it is a challenging task to find out larger symmetry groups which are automorphic to these remnant symmetries [3]. Nevertheless, for some predictive residual symmetries, a list of gauge groups has been addressed by C.S Lam [1] whereas the viability of Coexter group has been studied explicitly in Ref. [4]. Furthermore, to constrain the CP violating phases, in addition to a  $\mu\tau$ -interchange, a nonstandard CP transformation has also been proposed in Ref. [5]. Inspired by these well accepted road maps that redirect physicists towards the quest for an ultimate elusive model, in the present work we study the effect of a generalized  $\mathbb{Z}_2 \times \mathbb{Z}_2$  [6] that replicates scaling ansatz [7,8] in conjunction with a nonstandard CP transformation on light neutrino Majorana mass matrix.

We first consider a general neutrino mass matrix  $M_\nu^0$  having scaling ansatz as an effective low energy symmetry and following residual symmetry approach, interpret the latter as a residual  $\mathbb{Z}_2 \times \mathbb{Z}_2$  symmetry. Due to the outcome of a vanishing reactor angle  $\theta_{13}$  (which is excluded by experiment at more than  $5.2\sigma$  [9]), we further extend this symmetry with a CP transformation and demand a generalized  $\mathbb{Z}_2 \times \mathbb{Z}_2$  as an effective symmetry in the light neutrino mass term. In this case, having a more complicated scaling relationship between its elements, the resultant mass matrices (depending upon the ways of implementation of the symmetry, actually there are two light neutrino mass matrices) are further reconstructed through the type-I seesaw mechanism, by extending the SM with three right chiral singlet neutrino fields  $N_{iR}$  ( $i = 1, 2, 3$ ). Using the oscillation constraints, tantalizing predictions on the low energy parameters such as neutrino masses, neutrinoless double beta decay, CP violating phases are addressed. Due to the presence of three massive right handed (RH) neutrinos, baryogenesis

via leptogenesis scenario is also explored. Absorbing conclusions such as octant sensitivity of the atmospheric mixing angle  $\theta_{23}$ , preconditioned by the observed range of the final baryon asymmetry  $Y_B$  and nonoccurrence of unflavored leptogenesis are also drawn.

The paper is organized as follows. Section 2 contains a brief discussion on residual symmetry and scaling ansatz with a possible modification to the ansatz by extending the former with a nonstandard CP transformation. In Section 3 we discuss a type-I seesaw extension of the analysis made in the previous section. Section 4 contains a discussion about baryogenesis via leptogenesis scenario related to the present model. In Section 5 we present detail numerical results of the analysis. A discussion on the sensitivity of the heavier neutrinos to the obtained results for the final  $Y_B$  is presented in Section 6. Section 7 concludes the entire discussion with some promising remarks.

## 2 Modification to scaling neutrino mass matrix with generalized $\mathbb{Z}_2 \times \mathbb{Z}_2$

Before going to an explicit details of our work, let's first discuss the residual  $\mathbb{Z}_2 \times \mathbb{Z}_2$  symmetry proposed in Ref. [1]. A Majorana neutrino mass matrix  $M_\nu$  enjoys a  $\mathbb{Z}_2 \times \mathbb{Z}_2$  flavor symmetry which can be envisaged as a remnant symmetry of some horizontal flavor group. A linear transformation of the neutrino fields  $\nu_{L\alpha} \rightarrow G_{\alpha\beta}\nu_{L\beta}$  leads to an invariance of an effective neutrino Majorana mass term

$$-\mathcal{L}_{mass}^\nu = \frac{1}{2}\bar{\nu}_{L\alpha}^C(M_\nu)_{\alpha\beta}\nu_{L\beta} + h.c., \quad (2.1)$$

if the mass matrix  $M_\nu$  satisfies the invariance equation

$$G^T M_\nu G = M_\nu. \quad (2.2)$$

Here  $G$  is a  $3 \times 3$  unitary matrix in flavor with  $G^2 = I$ . Furthermore, since  $M_\nu$  is a complex symmetric matrix i.e.,  $M_\nu = M_\nu^T \neq M_\nu^*$ , it can be diagonalized by an unitary matrix  $U$  as

$$U^T M_\nu U = M_\nu^d = \text{diag}(m_1, m_2, m_3) \quad (2.3)$$

with  $m_{1,2,3}$  being real and positive. Eqs. 2.2 and 2.3 imply

$$(GU)^T M_\nu (GU) = M_\nu^d. \quad (2.4)$$

Therefore, if  $U$  diagonalizes  $M_\nu$  so does  $U' = GU$ . It can be shown that, if  $m_1, m_2$  and  $m_3$  are non-degenerate, then  $G$  has eigenvalues  $\pm 1$ , and is diagonalized by  $U$ . Thus one has

$$GU = Ud, \quad (2.5)$$

with

$$d^2 = I \quad (2.6)$$

where  $d$  is a  $3 \times 3$  diagonal matrix with elements  $d_{lm} = \pm\delta_{lm}$ . Clearly, there are eight possible choices for  $d$  among which only three are non-trivial<sup>1</sup>. Corresponding to these, there are three  $G_a$ 's ( $a = 1, 2, 3$ ) but only two of them are independent on account of the closure property  $G_a G_b = G_c$  with  $a \neq b \neq c$ . Moreover, it follows from Eqs. 2.5 and 2.6 that

$$G^2 = I, \quad \det G = \pm 1. \quad (2.7)$$

We may confine ourselves to the choice<sup>2</sup>  $\det G = +1$  and hence

$$d_1 = \text{diag}(1, -1, -1), \quad (2.8)$$

$$d_2 = \text{diag}(-1, 1, -1), \quad (2.9)$$

$$d_3 = \text{diag}(-1, -1, 1). \quad (2.10)$$

Thus given a mass matrix  $M_\nu$ , one can obtain  $U$  contingent with the symmetries of  $M_\nu$ . From which  $G'_a$ 's can be obtained as

$$G_a = U d_a U^\dagger \quad (2.11)$$

with  $a = 1, 2, 3$ . Basically for an arbitrary mixing matrix  $U$ , one can construct a unique  $G$ , however the reverse is not true due to the degeneracies in the eigenvalues of  $d_a$  matrices. From this point, the implementation of the residual symmetry to the neutrino mass matrix takes different paths. Given a leading order mixing matrix, e.g.  $U^{\mu\tau}$ , construction of  $G$  matrices are unique, then for a particular  $G$  matrix, one might or might not have  $U^{\mu\tau}$ . Papers such as [2] discuss scenarios like soft breaking of one of the two residual symmetries such that presence of the other with its degenerate eigenvalues enhances the degrees of choice of the mixing matrix in accordance with the phenomenological requirement. On the other hand, in Ref. [5, 6, 10], as a more predictive scenario, a CP transformation has been considered along with the  $\mu\tau$ -symmetry, without breaking the latter. Both the scheme have their own uniqueness in terms of the predictions on the low energy neutrino parameters. However, in this work, we follow the second one due to its robust predictions on CP violating phases which are related to the matter anti-matter asymmetry of the universe [11].

We interpret the Strong Scaling Ansatz (SSA) proposed in Ref. [7], as a residual  $\mathbb{Z}_2 \times \mathbb{Z}_2$  symmetry. Since SSA leads to a vanishing  $\theta_{13}$ , a possible modification to the former has been made by the inclusion of an additional CP transformation to the existing remnant symmetry. Let's discuss now the exact methodology of our analysis:

We consider a column wise scaling relations in the elements of  $M_\nu$  in flavor space as

$$\frac{(M_\nu^0)_{e\mu}}{(-M_\nu^0)_{e\tau}} = \frac{(M_\nu^0)_{\mu\mu}}{(-M_\nu^0)_{\mu\tau}} = \frac{(M_\nu^0)_{\tau\mu}}{(-M_\nu^0)_{\tau\tau}} = k, \quad (2.12)$$

---

<sup>1</sup>Two of them are trivial i.e.,  $d = \text{diag}(1, 1, 1)$  and  $d = \text{diag}(-1, -1, -1)$ . In the remaining six, three are negatives of the other three.

<sup>2</sup>The choice for the case  $\det G = -1$  is a trivial extension with  $d_i$  replaced with  $-d_i$ .

where  $k$  is a real and positive dimensionless scaling factor. The superscript ‘0’ on  $M_\nu$  symbolizes SSA as a leading order matrix in this analysis. Now the structure for  $M_\nu^0$  dictated by the ansatz of Eq. 2.12 comes out as

$$M_\nu^0 = \begin{pmatrix} P & -Qk & Q \\ -Qk & Rk^2 & -Rk \\ Q & -Rk & R \end{pmatrix}. \quad (2.13)$$

Here  $P, Q, R$  are complex mass dimensional quantities that are a priori unknown and the minus sign in Eq. (2.12) has been considered to be in conformity with the PDG convention [12]. The matrix in Eq. 2.13 is diagonalized by a unitary matrix  $U^0$  having a form

$$U^0 = \begin{pmatrix} c_{12}^0 & s_{12}^0 e^{i\alpha} & 0 \\ -\frac{ks_{12}^0}{\sqrt{1+k^2}} & \frac{kc_{12}^0}{\sqrt{1+k^2}} e^{i\alpha/2} & \frac{1}{\sqrt{1+k^2}} e^{i\beta/2} \\ \frac{s_{12}^0}{\sqrt{1+k^2}} & -\frac{c_{12}^0}{\sqrt{1+k^2}} e^{i\alpha/2} & \frac{k}{\sqrt{1+k^2}} e^{i\beta/2} \end{pmatrix} \quad (2.14)$$

where  $c_{12}^0 = \cos \theta_{12}^0$ ,  $s_{12}^0 = \sin \theta_{12}^0$  which are calculated in terms of the parameters of  $M_\nu^0$ , and  $\alpha, \beta$  represents the Majorana phases. SSA predicts a vanishing  $\theta_{13}$  (hence no measurable leptonic Dirac CP-violation) as one can see from Eq. (2.14) and an inverted neutrino mass ordering (i.e.,  $m_{2,1} > m_3$ ), with  $m_3 = 0$ . As previously mentioned, one needs to modify the ansatz to generate a non-zero  $\theta_{13}$ . Now using the residual symmetry approach as described in the previous section, one can calculate the  $G_a$  matrices using the relation

$$G_a^{(k)} = U^0 d_a U^{0\dagger} \quad (2.15)$$

with  $G_a^{(k)}$  as the  $\mathbb{Z}_2$  generators for a scaling ansatz invariant  $M_\nu$ . Similar to Eq. 2.2,  $M_\nu^0$  will then satisfy the invariance equation

$$(G_a^{(k)})^T M_\nu^0 G_a^{(k)} = M_\nu^0. \quad (2.16)$$

Now using Eq. 2.15 we calculate the corresponding  $G_a^{(k)}$  matrices and present them as

$$G_1^{(k)} = \begin{pmatrix} \cos 2\theta_{12}^0 & -k(1+k^2)^{-1/2} \sin 2\theta_{12}^0 & -(1+k^2)^{-1/2} \sin 2\theta_{12}^0 \\ -k(1+k^2)^{-1/2} \sin 2\theta_{12}^0 & -(1+k^2)^{-1} (k^2 \cos 2\theta_{12}^0 + 1) & -k(1+k^2)^{-1} (1 - \cos 2\theta_{12}^0) \\ -(1+k^2)^{-1/2} \sin 2\theta_{12}^0 & -k(1+k^2)^{-1} (1 - \cos 2\theta_{12}^0) & -(1+k^2)^{-1} (k^2 + \cos 2\theta_{12}^0) \end{pmatrix}, \quad (2.17)$$

$$G_2^{(k)} = \begin{pmatrix} -\cos 2\theta_{12}^0 & k(1+k^2)^{-1/2} \sin 2\theta_{12}^0 & -(1+k^2)^{-1/2} \sin 2\theta_{12}^0 \\ k(1+k^2)^{-1/2} \sin 2\theta_{12}^0 & (1+k^2)^{-1} (k^2 \cos 2\theta_{12}^0 - 1) & -k(1+k^2)^{-1} (1 + \cos 2\theta_{12}^0) \\ -(1+k^2)^{-1/2} \sin 2\theta_{12}^0 & -k(1+k^2)^{-1} (1 + \cos 2\theta_{12}^0) & -(1+k^2)^{-1} (k^2 - \cos 2\theta_{12}^0) \end{pmatrix}, \quad (2.18)$$

$$G_3^{(k)} = \begin{pmatrix} -1 & 0 & 0 \\ 0 & (1-k^2)(1+k^2)^{-1} & 2k(1+k^2)^{-1} \\ 0 & 2k(1+k^2)^{-1} & -(1-k^2)(1+k^2)^{-1} \end{pmatrix} \quad (2.19)$$

for  $a = 1, 2, 3$ . Now to modify SSA, we generalize this  $\mathbb{Z}_2 \times \mathbb{Z}_2$  with a CP transformation on the neutrino field [13] given as

$$\nu_{L\alpha} \rightarrow i(G_a^{(k)})_{\alpha\beta\gamma}{}^0 \nu_{L\beta}^C. \quad (2.20)$$

This extends the real horizontal invariance of  $M_\nu^0$  in Eq. 2.16 to its complex counterpart, i.e.

$$(G_a^{(k)})^T M_\nu G_a^{(k)} = M_\nu^*. \quad (2.21)$$

Therefore the SSA, elucidated as a  $\mathbb{Z}_2 \times \mathbb{Z}_2$  symmetry, has now been modified to an extended SSA, interpreted as a complex  $\mathbb{Z}_2 \times \mathbb{Z}_2$  symmetry which is some time also referred as a generalized  $\mathbb{Z}_2 \times \mathbb{Z}_2$  symmetry of  $M_\nu$  [6]. In the next subsections we show that there are only two ways in which such a complex extension can be done.

## 2.1 Case I: Complex extension of $G_{2,3}^{(k)}$ Invariance

The complex invariance relations of  $M_\nu$  related to  $G_{2,3}^{(k)}$  is now written as

$$(G_{2,3}^{(k)})^T M_\nu G_{2,3}^{(k)} = M_\nu^*, \quad (2.22)$$

which in turn implies

$$(G_1^{(k)})^T M_\nu G_1^{(k)} = M_\nu \quad (2.23)$$

owing to the closure property of the  $G_a^{(k)}$  ( $a = 1, 2, 3$ ) matrices.

Eq. 2.22 leads to a most general Majorana neutrino mass matrix of the form

$$M_\nu^{MS1} = \begin{pmatrix} p & -q_1 k + i \frac{q_2}{k} & q_1 + i q_2 \\ -q_1 k + i \frac{q_2}{k} & r - \frac{s(k^2-1)}{k} + i \frac{2q_2 \kappa_+}{\sqrt{1+k^2}} & s + i \frac{q_2 \kappa_+(k^2-1)}{k\sqrt{1+k^2}} \\ q_1 + i q_2 & s + i \frac{q_2 \kappa_+(k^2-1)}{k\sqrt{1+k^2}} & r - i \frac{2q_2 \kappa_+}{\sqrt{1+k^2}} \end{pmatrix} \quad (2.24)$$

with

$$r = (sk + p) - q_1 \sqrt{1+k^2} \left( \kappa_+ - \frac{1}{\kappa_+} \right), \quad (2.25)$$

$$\kappa_+ = (\cot 2\theta_{12}^0 + \operatorname{cosec} 2\theta_{12}^0). \quad (2.26)$$

Here  $p$ ,  $q_{1,2}$ ,  $r$  and  $s$  are real, mass dimensional quantities. It has already been shown in Ref. [14] that  $(G_3^{(k)})^T M_\nu G_3^{(k)} = M_\nu^*$  leads to the results

$$\tan \theta_{23} = k^{-1}, \quad (2.27)$$

$$\sin \alpha = \sin \beta = \cos \delta = 0. \quad (2.28)$$

Now in the present case, the overall real  $G_1$  (cf. Eq.2.23) invariance of  $M_\nu$  fixes the first column of  $U_{PMNS}$  to the first column of  $U^0$ . Therefore, one gets the relation between the solar and the reactor mixing angle as

$$|\cos \theta_{12} \cos \theta_{13}| = \cos \theta_{12}^0 \Rightarrow \sin^2 \theta_{12} = 1 - \cos^2 \theta_{12}^0 (1 + \tan^2 \theta_{13}). \quad (2.29)$$

## 2.2 Case II: Complex extension of $G_{1,3}^{(k)}$ Invariance

In this case, the complex invariance relations of  $M_\nu$  due to  $G_{1,3}^{(k)}$  can be written as

$$(G_{1,3}^{(k)})^T M_\nu G_{1,3}^{(k)} = M_\nu^*, \quad (2.30)$$

which leads to

$$(G_2^{(k)})^T M_\nu G_2^{(k)} = M_\nu. \quad (2.31)$$

Eq. 2.30 leads to the mass matrix  $M_\nu^{MS2}$  having a form same as  $M_\nu^{MS1}$  as given in Eq. (2.24) where  $\kappa_+$  is replaced with  $\kappa_- = -1/\kappa_+$ . Now the overall real  $G_2$  (cf. Eq. 2.31) invariance of  $M_\nu$  fixes the second column of  $U_{PMNS}$  to the second column of  $U^0$ . Therefore, one gets the relation between the solar and the reactor mixing angle as

$$|\sin \theta_{12} \cos \theta_{13}| = \sin \theta_{12}^0 \Rightarrow \sin^2 \theta_{12} = \sin^2 \theta_{12}^0 (1 + \tan^2 \theta_{13}). \quad (2.32)$$

## 2.3 Case III: Complex extension of $G_{1,2}^{(k)}$ Invariance

Similar to the previous cases, the complex invariance relations of  $M_\nu$  related to  $G_{1,2}^{(k)}$  can be written as

$$(G_{1,2}^{(k)})^T M_\nu G_{1,2}^{(k)} = M_\nu^*, \quad (2.33)$$

which in turn implies

$$(G_3^{(k)})^T M_\nu G_3^{(k)} = M_\nu. \quad (2.34)$$

However, since  $G_3^{(k)}$  fixes the third column of  $U_{PMNS}$  to the third column of  $U^0$ , this invariance leads to a vanishing value of  $\theta_{13}$ . Thus simultaneous complex invariance of  $M_\nu$  due to  $G_1^{(k)}$  and  $G_2^{(k)}$ , is not a viable extension of SSA.

Resolving the shortcomings of SSA, both the viable modified SSA matrices possess intriguing phenomenology. This has been discussed in the numerical section of the analysis. For the time being let's focus on the implementation of the symmetry in a more specific way. So far we have discussed a possible complex extension for a general  $M_\nu$ , not so about the origin of the neutrino masses. This would be interesting to see the effects of generalized  $\mathbb{Z}_2 \times \mathbb{Z}_2$  on a particular mechanism that generates the light neutrino masses. Obviously, the choice depends upon the phenomenological interest. Here we choose the type-I seesaw mechanism and investigate possible consequences of the generalized  $\mathbb{Z}_2 \times \mathbb{Z}_2$  to explore the phenomena of baryogenesis via leptogenesis. A detailed discussion about these has been presented in the next two sections. First, we show the reconstruction of the effective modified SSA matrices through type-I seesaw mechanism with proper implementation of the symmetry on the constituent matrices ( $m_D$  and  $M_R$ ). Then we discuss some aspects of baryogenesis via leptogenesis related to this scheme.

### 3 Reconstruction of modified scaling matrices with type-I seesaw

For the realization of generalized  $\mathbb{Z}_2 \times \mathbb{Z}_2$  in the context of type-I seesaw mechanism, we define two separate ‘G’ matrices  $G_L$  and  $G_R$  for  $\nu_L$  and  $N_R$  fields respectively. Now the CP transformations are defined on these fields as [15]

$$\nu_{L\alpha} \rightarrow i(G_L)_{\alpha\beta}\gamma^0\nu_{L\beta}^C, \quad N_{R\alpha} \rightarrow i(G_R)_{\alpha\beta}\gamma^0N_{R\beta}^C. \quad (3.1)$$

With  $m_D$  as a Dirac type and  $M_R$  as a diagonal nondegenerate Majorana type mass matrix, the Lagrangian for type-I seesaw

$$-\mathcal{L}_{mass} = \bar{N}_{lR}(m_D)_{l\alpha}L_\alpha + \frac{1}{2}\bar{N}_{lR}(M_R)_l\delta_{lm}N_{mR}^C + \text{h.c.} \quad (3.2)$$

leads to the effective light neutrino  $3 \times 3$  Majorana mass matrix  $M_\nu$  as

$$M_\nu = -m_D^T M_R^{-1} m_D. \quad (3.3)$$

Now the invariance of the mass terms of (3.2) under the CP transformations defined in (3.1) leads to the relations

$$G_R^\dagger m_D G_L = m_D^*, \quad G_R^\dagger M_R G_R^* = M_R^*. \quad (3.4)$$

Eqs. (3.3) and (3.4) together imply  $G_L^T M_\nu G_L = M_\nu^*$ . Now, specifying  $G_L$  by  $G_i^{(k)}$ , we obtain the key equation

$$(G_i^{(k)})^T M_\nu G_i^{(k)} = M_\nu^*. \quad (3.5)$$

Since  $M_R$  is taken to be diagonal i.e.,  $M_R = \text{diag}(M_1, M_2, M_3)$ , the corresponding symmetry generator matrix  $G_R$  is diagonal [15] with entries  $\pm 1$ , i.e.,

$$(G_R)_{lm} = \pm\delta_{lm}. \quad (3.6)$$

which implies for each  $G_L$ , there are eight different structures for  $G_R$  that correspond to eight different choices of  $m_D$ . However, a straightforward computation shows that for the case-I, the  $G_R$  matrix compatible with  $G_2^{(k)}$  and  $G_3^{(k)}$  should be taken as  $(G_R)_2 = \text{diag}(1, 1, 1)$  and  $(G_R)_3 = \text{diag}(-1, -1, -1)$  respectively. Similarly for Case-II also, those are taken as  $(G_R)_1 = \text{diag}(1, 1, 1)$  and  $(G_R)_3 = \text{diag}(-1, -1, -1)$  for  $G_1^{(k)}$  and  $G_3^{(k)}$ . It can be shown that all the other choices of  $G_R$  are incompatible with scaling symmetry. Therefore, the first of Eq. 3.4 leads to

$$\begin{aligned} m_D G_3 &= -m_D^*, m_D G_2 = m_D^* && \text{for Case-I} \\ m_D G_3 &= -m_D^*, m_D G_1 = m_D^* && \text{for Case-II.} \end{aligned} \quad (3.7)$$



For both the cases as discussed above, the most general form of  $m_D$  that satisfies the constraints of Eq.(3.7) can be parameterized as

$$m_D^{MS} = \begin{pmatrix} a & b_1 + ib_2 & -b_1/k + ib_2k \\ e & c_1 + ic_2 & -c_1/k + ic_2k \\ f & d_1 + id_2 & -d_1/k + id_2k \end{pmatrix} \quad (3.8)$$

with

$$b_1 = \pm ak(1 + k^2)^{-1/2}\kappa_{\pm}, \quad (3.9)$$

$$c_1 = \pm ek(1 + k^2)^{-1/2}\kappa_{\pm}, \quad (3.10)$$

$$d_1 = \pm fk(1 + k^2)^{-1/2}\kappa_{\pm}. \quad (3.11)$$

Here the ‘ $\pm$ ’ sign in the expressions of  $b_1, c_1$  and  $d_1$  are for Case-I and Case-II respectively. In Eq. 3.8  $a, e, f, b_2, c_2$  and  $d_2$  are six a priori unknown real mass dimensional quantities apart from the real, positive, dimensionless  $k$ . Now using the seesaw relation in Eq. 3.3, it is easy to reconstruct the effective mass matrices  $M_{\nu}^{MS1}$  and  $M_{\nu}^{MS2}$  for Case-I and Case-II respectively. In Table 1 we present the parameters of the effective light neutrino mass matrix in terms of the Dirac and Majorana components.

Table 1: Parameters of  $M_{\nu}$

$$\begin{aligned} p &= -\left(\frac{a^2}{M_1} + \frac{e^2}{M_2} + \frac{f^2}{M_3}\right) \\ q_1 &= -\frac{\kappa_{\pm}p}{\sqrt{1+k^2}} \\ q_2 &= -k\left(\frac{ab_2}{M_1} + \frac{ec_2}{M_2} + \frac{fd_2}{M_3}\right) \\ s &= -\frac{\kappa_{\pm}pk}{1+k^2} + k\left(\frac{b_2^2}{M_1} + \frac{c_2^2}{M_2} + \frac{d_2^2}{M_3}\right) \\ r &= (sk + p) - q_1\sqrt{1+k^2}\left(\kappa_{\pm} - \frac{1}{\kappa_{\pm}}\right) \end{aligned}$$

Once again ‘ $\pm$ ’ sign in  $\kappa$  are for Case-I and Case-II respectively.

## 4 Baryogenesis via leptogenesis

Baryogenesis via leptogenesis [16, 17] is a phenomena where CP violating and out of equilibrium decays from heavy Majorana neutrinos creates an lepton asymmetry which is thereafter converted into baryon asymmetry by sphaleronic transition [18]. The pertinent Lagrangian for the process can be written as

$$-\mathcal{L}_D = \lambda_{i\alpha}\bar{N}_{Ri}\tilde{\phi}^{\dagger}l_{L\alpha} + h.c. \quad (4.1)$$

where  $l_{L\alpha} = \left(\nu_{L\alpha} \ e_{L\alpha}\right)^T$  is the SM lepton doublet of flavor  $\alpha$ , and  $\tilde{\phi} = i\tau_2\phi^*$  with  $\phi = \left(\phi^+ \ \phi^0\right)^T$  being the Higgs doublet. Thus the possible decays of  $N_i$  from 4.1 are  $N_i \rightarrow e_{\alpha}^{-}\phi^+$ ,

$N_i \rightarrow \nu_\alpha \phi^0$ ,  $N_i \rightarrow e_\alpha^+ \phi^-$ , and  $N_i \rightarrow \nu_\alpha^C \phi^{0*}$ . The CP asymmetry parameter  $\varepsilon_i^\alpha$  that accounts for the required CP violation, arises due to the interference between the tree level, one loop self energy, one loop vertex  $N_i$ -decay diagrams [16] and has a general expression [19]

$$\varepsilon_i^\alpha = \frac{1}{4\pi v^2 h_{ii}} \sum_{j \neq i} \left\{ \text{Im}[h_{ij}(m_D)_{i\alpha}(m_D^*)_{j\alpha}]g(x_{ij}) + \frac{\text{Im}[h_{ji}(m_D)_{i\alpha}(m_D^*)_{j\alpha}]}{1 - x_{ij}} \right\} \quad (4.2)$$

where  $h \equiv m_D m_D^\dagger$ ,  $\langle \phi^0 \rangle = v/\sqrt{2}$  so that  $m_D = v\lambda/\sqrt{2}$ , and  $x_{ij} = M_j^2/M_i^2$ . Furthermore, the loop function  $g(x_{ij})$  has the expression

$$g(x_{ij}) = \frac{\sqrt{x_{ij}}}{1 - x_{ij}} + f(x_{ij}) \quad (4.3)$$

with

$$f(x_{ij}) = \sqrt{x_{ij}} \left[ 1 - (1 + x_{ij}) \left( \ln \frac{1 + x_{ij}}{x_{ij}} \right) \right]. \quad (4.4)$$

Before going to the explicit calculation of  $\varepsilon_i^\alpha$  related to this model, let's address some important issues related to leptogenesis. For a hierarchical scenario, e.g.,  $M_3 \gg M_2 \gg M_1$ , it can be shown that only the decays of  $N_1$  matter for the creation of lepton asymmetry while the latter created from the heavier neutrinos get washed out [20]. Obviously there are certain circumstances when the decays of  $N_{2,3}$  are also significant [21]. Again, flavor plays an important role in the phenomena of leptogenesis [22]. Assuming the temperature scale of the process  $T \sim M_1$ , the rates of the Yukawa interaction categorize leptogenesis into three categories. I)  $T \sim M_1 > 10^{12}$  GeV, when all interactions with all flavors are out of equilibrium: unflavored leptogenesis. In this case all the flavors are indistinguishable and thus the total CP asymmetry is a sum over individual flavor;  $\varepsilon_i = \sum_\alpha \varepsilon_i^\alpha$ . II)  $10^9$  GeV  $< T \sim M_1 < 10^{12}$  GeV, when only the  $\tau$  flavor are in equilibrium:  $\tau$ -flavored leptogenesis. In this regime there are two relevant CP asymmetry parameters;  $\varepsilon_i^\tau$  and  $\varepsilon_i^2 = \varepsilon_i^e + \varepsilon_i^\mu$ . III)  $T \sim M_1 < 10^9$  GeV, when all the flavors ( $e, \mu, \tau$ ) are in equilibrium and distinguishable: fully flavored leptogenesis.

In our model, the flavor sum on  $\alpha$  leads to a vanishing value of the second term in Eq. 4.2, since

$$\sum_\alpha \text{Im}[h_{ji}(m_D)_{i\alpha}(m_D^*)_{j\alpha}] = \text{Im}[h_{ji}h_{ij}] = \text{Im}|h_{ji}|^2 = 0, \quad (4.5)$$

while the first term is proportional to  $\text{Im}(h^\dagger h)_{ij}$ . Now for both the cases in our model,  $h$  has a generic form

$$h = \begin{pmatrix} a^2(1 + \kappa_\pm^2) + b_2^2(1 + k^2) & ae(1 + \kappa_\pm^2) + (1 + k^2)b_2c_2 & af(1 + \kappa_\pm^2) + (1 + k^2)b_2d_2 \\ ae(1 + \kappa_\pm^2) + (1 + k^2)b_2c_2 & e^2(1 + \kappa_\pm^2) + c_2^2(1 + k^2) & ef(1 + \kappa_\pm^2) + (1 + k^2)c_2d_2 \\ af(1 + \kappa_\pm^2) + (1 + k^2)b_2d_2 & ef(1 + \kappa_\pm^2) + (1 + k^2)c_2d_2 & f^2(1 + \kappa_\pm^2) + d_2^2(1 + k^2) \end{pmatrix} \quad (4.6)$$

with '±' sign in  $\kappa$  are for Case-I and Case-II respectively. Note that the matrix  $h$  in Eq. 4.6 is real. Therefore, unflavored leptogenesis which is relevant for the high temperature regime

does not take place for any  $N_i$  in this model. With the assumption that only the decay of  $N_1$  matters in generating the CP asymmetry,  $\varepsilon_1$  is the relevant quantity for unflavored leptogenesis, but it vanishes in this model.

Next, we concentrate on computing the  $\alpha$ -flavored CP asymmetry in terms of  $x_{12}$ ,  $x_{13}$  and the elements of  $m_D$ . These are necessary ingredients for the fully flavored and the  $\tau$ -flavored regimes. We find a vanishing value for  $\varepsilon_1^e$  while  $\varepsilon_1^{\mu,\tau}$  are calculated as

$$\varepsilon_1^\mu = \zeta[b_2k^2(\chi_1 + \chi_2) + b_1(\chi_3 + \chi_4) - b_2\chi_5] = -\varepsilon_1^\tau. \quad (4.7)$$

In 4.7 the real parameters  $\zeta$  and  $\chi_i$  ( $i = 1 - 5$ ) are defined as

$$\zeta = [4\pi v^2(b_1^2 + (a^2 + b_1^2 + b_2^2)k^2 + b_2k^4)]^{-1}, \quad (4.8)$$

$$\chi_1 = b_2(1 + k^2)[c_1c_2A_{12} + d_1d_2A_{13}], \quad (4.9)$$

$$\chi_2 = c[c_1eA_{12} + d_1fA_{13}], \quad (4.10)$$

$$\chi_3 = b_2(1 + k^2)[c_1^2A_{12} - k^2(c_2^2A_{12} - d_2^2A_{13}) + d_1^2A_{13}], \quad (4.11)$$

$$\chi_4 = -ak^2[c_2eA_{12} + d_2fA_{13}], \quad (4.12)$$

$$\chi_5 = (1 + k^2)[c_1c_2A_{12} + d_1d_2A_{13}]. \quad (4.13)$$

where  $A_{ij} = g(x_{ij}) + (1 - x_{ij})^{-1}$ . Now the final baryon asymmetry for  $10^9 \text{ GeV} < T \sim M_1 < 10^{12} \text{ GeV}$  and  $T \sim M_1 < 10^9 \text{ GeV}$  regime are well approximated with [22]

$$Y_B \simeq -\frac{12}{37g^*} \left[ \varepsilon_i^{(2)} \eta \left( \frac{417}{589} \tilde{m}_2 \right) + \varepsilon_i^{(\tau)} \eta \left( \frac{390}{589} \tilde{m}_\tau \right) \right] \quad (4.14)$$

and

$$Y_B \simeq -\frac{12}{37g^*} \left[ \varepsilon_i^{(e)} \eta \left( \frac{151}{179} \tilde{m}_e \right) + \varepsilon_i^{(\mu)} \eta \left( \frac{344}{537} \tilde{m}_\mu \right) + \varepsilon_i^{(\tau)} \eta \left( \frac{344}{537} \tilde{m}_\tau \right) \right] \quad (4.15)$$

respectively, where  $\tilde{m}_\alpha$  is the wash-out mass, defined as

$$\tilde{m}_\alpha = \frac{|(m_D)_{1\alpha}|^2}{M_1} \quad (4.16)$$

and  $\eta(\tilde{m}_\alpha)$  is the efficiency factor that accounts for the inverse decay and the lepton number violating scattering process along with an explicit dependence upon the wash-out regimes under consideration.

## 5 Numerical analysis: methodology and discussion

In order to assess the viability of our theoretical conjecture and consequent outcomes, we present a numerical analysis in substantial detail for both the viable cases. Our method of analysis and organization are as follows. First, we utilize the  $(3\sigma)$  values of globally fitted

neutrino oscillation data (Table 2), together with an upper bound of 0.23 eV on the sum of the light neutrino masses from PLANCK and other cosmological observations to constrain the parameter space in terms of the rescaled (primed) parameters defined below.

$$\begin{aligned}
a &\longrightarrow a' = \frac{a}{\sqrt{M_1}}, e \longrightarrow e' = \frac{e}{\sqrt{M_2}}, \\
f &\longrightarrow f' = \frac{f}{\sqrt{M_2}}, b_{1,2} \longrightarrow b'_{1,2} = \frac{b_{1,2}}{\sqrt{M_1}}, \\
c_{1,2} &\longrightarrow c'_{1,2} = \frac{c_{1,2}}{\sqrt{M_2}}, d_{1,2} \longrightarrow d'_{1,2} = \frac{d_{1,2}}{\sqrt{M_3}}.
\end{aligned} \tag{5.1}$$

Then we explore the predictions of the present model in the context of the  $\beta\beta_{0\nu}$  experiments for each of the cases. Finally, in order to estimate the value of  $Y_B$  we make use of these constrained parameters with a subtlety. Since we have only constrained the primed parameters, there remains a freedom of various set of independent choices for the parameters of  $m_D$  (unprimed) along with  $M_i$ , for a given set of primed parameters. Note that for the computation of  $Y_B$  we need to feed the unprimed parameters and  $M_i$  separately. However for the entire parameter space of primed parameters, it is impractical to generate the unprimed ones for different values of  $M_i$ s as one ends up with an infinite number of choices. For this, we have considered only those set of primed parameters that are close to their best-fit values dictated by the oscillation data. Then varying  $M_1$ , we generate the corresponding unprimed set. Computing baryon asymmetry thereafter for each primed set— thus for corresponding values unprimed parameters and  $M_i$ s, we emphasize our final result for that primed data set which is closest to the best-fit point as well as results in a positive value of  $Y_B$  within the observed range. Now let's have an elaborate numerical discussion one by one as introduced in this section.

### Constraints from oscillation data

For each of the viable cases, both the normal and inverted hierarchy of light neutrino masses are found to be permitted over a respectable size of parameter space consistent with the aforementioned experimental constraints. The ranges of the rescaled parameters for both the cases I and II are graphically shown in Fig. 1-4. In both the cases, reduction in the number

Table 2: Input values fed into the analysis [23]

Parameters degrees	$\theta_{12}$ degrees	$\theta_{23}$ degrees	$\theta_{13}$ $10^{-5}\text{eV}^2$	$\Delta m_{21}^2$ $10^{-3}(\text{eV}^2)$	$ \Delta m_{31}^2 $ (eV)
$3\sigma$ ranges/ others	31.29 – 35.91	38.3 – 53.3	7.87 – 9.11	7.02 – 8.09	2.32 – 2.59
Best fit values (NO)	33.48	42.3	8.50	7.50	2.46
Best fit values (IO)	33.48	49.5	8.51	7.50	2.45

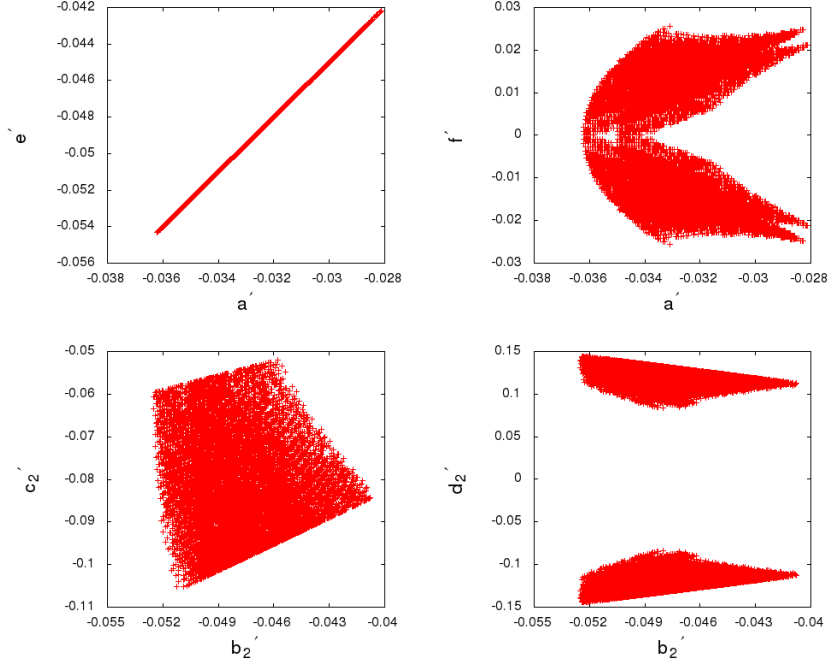


Figure 1: Case-I: Plots of the rescaled parameters for a normal mass hierarchy.

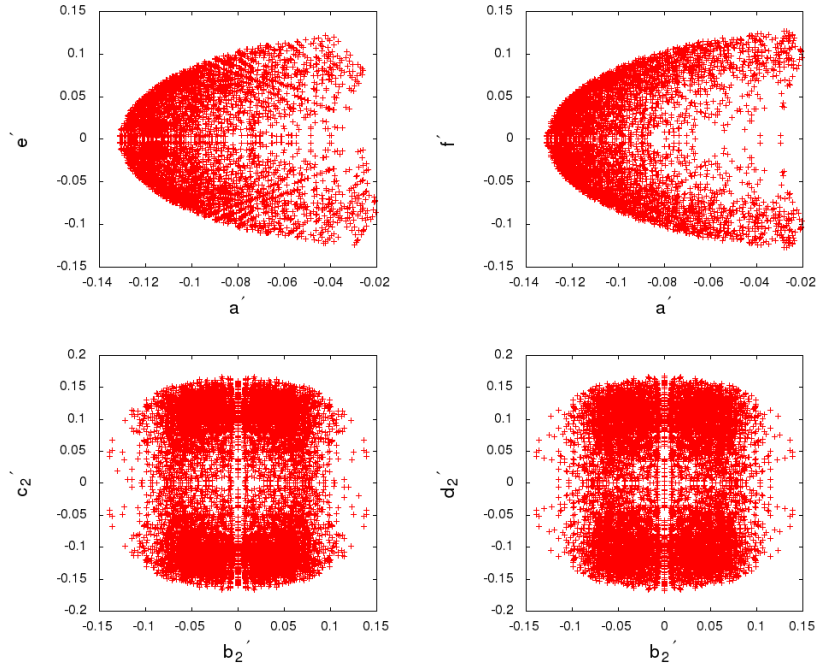


Figure 2: Case-I: Plots of the rescaled parameters for a inverted mass hierarchy.

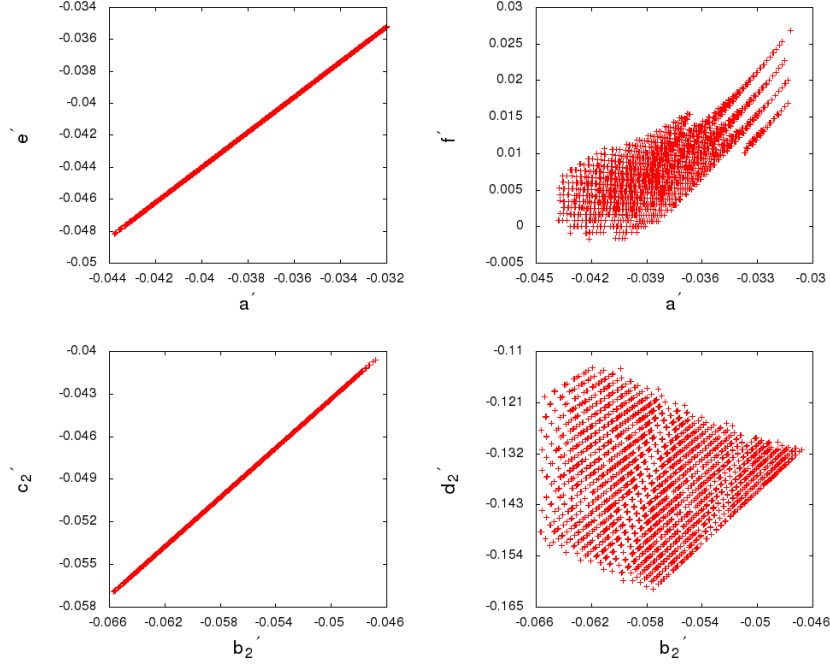


Figure 3: Case-II: Plots of the rescaled parameters for a normal mass hierarchy.

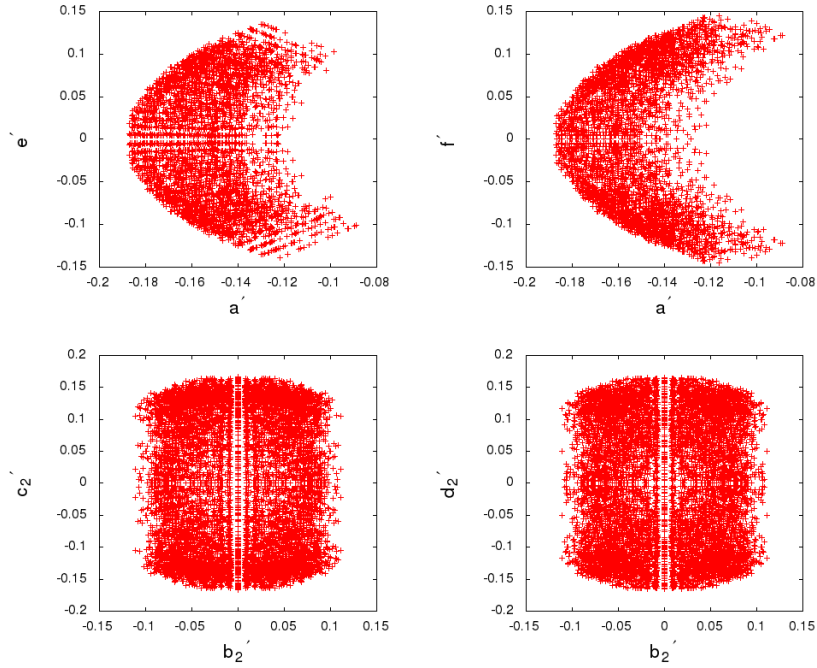


Figure 4: Case-II: Plots of the rescaled parameters for a normal mass hierarchy.

of parameters upon rescaling led to a constrained range for each of the light neutrino masses as

depicted in Table 3. It has been found that all the light neutrino mass spectrum are hierarchical. Interestingly, though the upper bound on  $\sum_i m_i$  is fed in as an input constraint, the bound has not been reached up in our model irrespective of the mass ordering. The predictions on  $\sum_i m_i$  are tabulated in Table 3 for each of the cases.

Table 3: Predictions on the light neutrino masses and  $\sum_i m_i$

Case-I					
Normal Ordering			Inverted Ordering		
$m_1/10^{-3}$ (eV)	$m_2/10^{-3}$ (eV)	$m_3/10^{-3}$ (eV)	$m_1/10^{-3}$ (eV)	$m_2/10^{-3}$ (eV)	$m_3/10^{-3}$ (eV)
4.0 – 8.5	9.28 – 12.0	49 – 52	47 – 61	–49 – 62	9 – 36
$\sum_i m_i < 0.08$ eV			$\sum_i m_i < 0.16$ eV		
Case-II					
Normal Ordering			Inverted Ordering		
$m_1/10^{-3}$ (eV)	$m_2/10^{-3}$ (eV)	$m_3/10^{-3}$ (eV)	$m_1/10^{-3}$ (eV)	$m_2/10^{-3}$ (eV)	$m_3/10^{-3}$ (eV)
4.1 – 8.8	9.23 – 13.1	48 – 52	47 – 60	49 – 61	10 – 38
$\sum_i m_i < 0.08$ eV			$\sum_i m_i < 0.16$ eV		

### Neutrinoless double beta decay $0\nu\beta\beta$

This is a process arising from the decay of a nucleus as

$$(A, Z) \longrightarrow (A, Z + 2) + 2e^- \quad (5.2)$$

where the lepton number is violated by 2 units due to the absence of any final state neutrinos. Observation of such decay will lead to the confirmation of the Majorana nature of the neutrinos. The half-life [25] corresponding to the above decay is given by

$$\frac{1}{T_{1/2}^{0\nu}} = G|\mathcal{M}|^2|M_{ee}|^2m_e^{-2}, \quad (5.3)$$

where  $G$  is the two-body phase space factor,  $\mathcal{M}$  is the nuclear matrix element (NME),  $m_e$  is the mass of the electron and  $M_{ee}$  is the (1,1) element of the effective light neutrino mass matrix  $M_\nu$ . Using the PDG parametrization convention for  $U_{PMNS}$  [12], the  $M_{ee}$  can be written as

$$M_{ee} = c_{12}^2 c_{13}^2 m_1 + s_{12}^2 c_{13}^2 m_2 e^{i\alpha} + s_{13}^2 m_3 e^{i(\beta-2\delta)}. \quad (5.4)$$

Significant upper limits on  $|M_{ee}|$  are available from several ongoing experiments. Experiments such as KamLAND-Zen [27] and EXO [26] have constrained this value to be  $< 0.35$  eV. However, till date the most impressive upper bound of 0.22 eV on  $|M_{ee}|$  is provided by GERDA

phase-I data [28] which is likely to be lowered even further by GERDA phase -II data [29] to around 0.098 eV.

As shown in Ref. [14], existence of  $G_3^{(k)}$  in the neutrino mass matrix leads to four sets of values of the CP-violating Majorana phases  $\alpha$  and  $\beta$  for each neutrino mass ordering. Since  $|M_{ee}|$  is sensitive to these phases, we get four different plots for each mass ordering. In Fig. 5 we show the  $|M_{ee}|$  vs. the lightest neutrino mass ( $m_{1,3}$ ) plot for both the mass orderings for case-I only. Case-II also leads to similar plots apart from a slight change in the upper and lower limits on  $m_{1,3}$ .

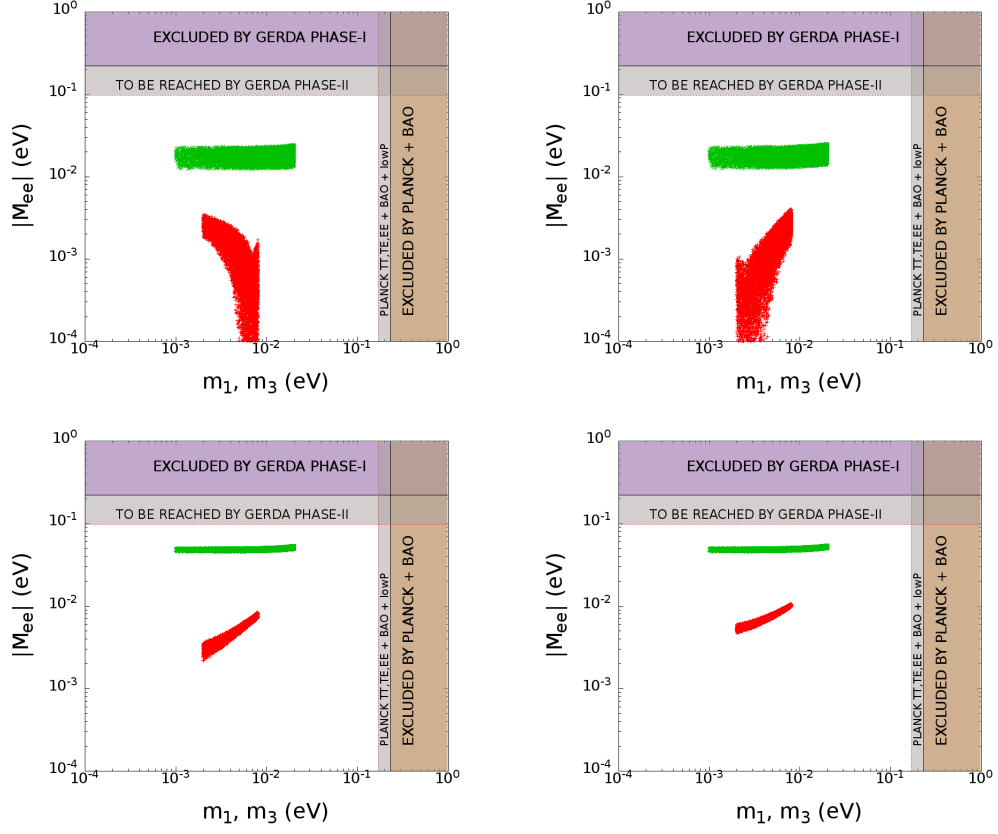


Figure 5: Plot of  $|M_{ee}|$  vs. the lightest neutrino mass: the top two figures represent Case A:  $\alpha = \pi$ ,  $\beta = 0$  (left) and Case B:  $\alpha = \pi$ ,  $\beta = \pi$  (right) while the figures in the lower panel represent Case C:  $\alpha = 0$ ,  $\beta = 0$  (left) and Case D:  $\alpha = 0$ ,  $\beta = \pi$  (right).

This is evident from Fig. 5 that  $|M_{ee}|$  in each plot leads to an upper limit which is below the reach of the GERDA phase-II data. However predictions of our model could be probed by GERDA + MAJORANA experiments [30]. One can also explain the nature of the plots analytically. Let us first consider the inverted mass ordering: In this case, with the



approximations  $m_3 \simeq 0$  and  $m_1 \simeq m_2$ , the effective mass  $|M_{ee}|$  simplifies to

$$|M_{ee}| = \sqrt{|\Delta m_{32}|^2 c_{13}^2 [\{1 - s_{12}^2(1 - \cos \alpha)\}^2 + s_{12}^4 \sin^2 \alpha]^{1/2}}. \quad (5.5)$$

Clearly,  $|M_{ee}|$  is not sensitive to the phases  $\beta$  and  $\delta$ . On the other hand, for  $\alpha = \pi$  and 0 (5.5) simplifies to

$$|M_{ee}| = \sqrt{|\Delta m_{32}|^2 c_{13}^2 [\{1 - 2s_{12}^2\}^2]} \quad (5.6)$$

and

$$|M_{ee}| = \sqrt{|\Delta m_{32}|^2 c_{13}^2} \quad (5.7)$$

respectively. Therefore, for  $\alpha = \pi$  (cases A, B),  $|M_{ee}|$  is suppressed as compared to the case  $\alpha = 0$  (C, D). Now for a normal mass ordering, in addition to the  $s_{13}$  suppression, there is a significant interference between the first two terms. If  $\alpha = 0$ , the first two terms interfere constructively and we obtain a lower bound ( $\sim 10^{-3}$  eV for Case C and  $\sim 5 \times 10^{-3}$  eV for Case D) despite it being a case of normal mass ordering of the light neutrinos. This is one of the crucial results of the present analysis. On the other hand, for  $\alpha = \pi$ , the first two terms interfere destructively and thus a sizable cancellation between them brings down the value of  $|M_{ee}|$  and results in the kinks that is depicted in the lower curves in the top two figures.

#### Baryogenesis via flavored leptogenesis:

As mentioned in the beginning of the numerical section, constraining the rescaled (primed) parameters from the neutrino oscillation data is only a primary restriction. For a particular value of primed parameter, one might generate a huge number of unprimed parameters by varying  $M_i$  over a wide range. However, for the computational purpose, this is impractical to generate enormous amount of unprimed parameters by varying  $M_i$  for the entire allowed region of the rescaled parameters. So to get a positive  $Y_B$ , we were obliged to use those value of the rescaled parameters for which the low energy neutrino parameters predicted from our model lie close to their best fit values dictated by the oscillation experiment. To facilitate this purpose, we define a variable  $\chi^2$  in Eq. (5.8) that measure deviation of the parameters from their best fit values.

$$\chi^2 = \sum_{i=1}^5 \left[ \frac{\mathcal{O}_i(th) - \mathcal{O}_i(bf)}{\Delta \mathcal{O}_i} \right]^2. \quad (5.8)$$

In (5.8)  $\mathcal{O}_i$  denotes the  $i$ th neutrino oscillation observable among  $\Delta m_{21}^2, \Delta m_{32}^2, \theta_{12}, \theta_{23}$  and  $\theta_{13}$  and the summation runs over all of them. The parenthetical *th* stands for the numerical value of the observable given by our model, whereas *bf* denotes the best fit value (cf. Table 2).  $\Delta \mathcal{O}_i$  in the denominator stands for the measured  $1\sigma$  range of  $\mathcal{O}_i$ . For numerical computation, we choose  $M_{i+1}/M_i = 10^3$  ( $i = 1, 2$ )<sup>3</sup>. First we calculate  $\chi^2$  in the as a function of the primed

<sup>3</sup>In the next section a detailed discussion is given regarding the sensitivity of  $Y_B$  to the chosen hierarchy of  $M_i$ .

parameters in their constrained range. Next we start with the minimum value of  $\chi^2$  and keep on increasing it until  $Y_B$  attains a positive value. For that particular  $\chi^2$  i.e., a particular set of primed parameters, we are able to generate a large set of unprimed parameters by varying  $M_1$  over a wide range. Using the observed range of  $Y_B$  we put an upper and lower bound on  $M_1$ . For each case here under consideration, we do this analysis in the relevant mass regimes for both types of mass ordering and present our final result systematically in the following way.

**Case-I:  $Y_B$  for normal mass ordering of light neutrinos:**

**$M_1 < 10^9$  GeV:** In this regime, all three lepton flavors ( $e, \mu, \tau$ ) are distinguishable. Since  $\varepsilon_1^e = 0$ , we need to individually evaluate  $\varepsilon_1^{\mu, \tau}$  only. Numerically, the maximum value of  $|\varepsilon_1^{\mu, \tau}|$  is found to be  $\sim 10^{-8}$ .  $Y_B$  in the observed range cannot be generated with such a small CP asymmetry parameter. Theoretically, this can be understood as an interplay between various quantities. A unique feature in the present model is that the nonzero value of  $\theta_{13}$  and  $\varepsilon_i$  originated from the imaginary part of the  $m_D$  matrix. A lower value of  $k$  is needed to fix the value of  $\theta_{13}$  which in turn depletes the value of  $\varepsilon$  in this regime.

**$10^9$  GeV  $< M_1 < 10^{12}$  GeV:** Before calculating final  $Y_B$ , we have to look first at the wash-out parameters  $K_\alpha = \tilde{m}_\alpha/10^{-3}$  relevant to this mass regime. Since in this regime only  $\tau$  flavor is distinguishable, there are two wash-out parameters,  $K_\tau$  and  $K_2 = K_e + K_\mu$ . As shown in the first plot of Fig. 6, the entire range these parameters is not much greater than 1 for the observed range of  $Y_B$ . Thus the efficiency factor in Eq (4.14) can be written for this mild wash-out scenario [22] as

$$\eta(\tilde{m}_\alpha) = \left[ \left( \frac{\tilde{m}_\alpha}{8.25 \times 10^{-3}} \right)^{-1} + \left( \frac{0.2 \times 10^{-3}}{\tilde{m}_\alpha} \right)^{-1.16} \right]^{-1}. \quad (5.9)$$

We then perform a  $\chi^2$  scanning of the rescaled parameters. It has been found that for  $\chi_{min}^2 = 0.083$  one can have  $Y_B$  positive. A complete data set of the rescaled parameters is tabulated in Table 4. The other parameters i.e.,  $b_1, c_1, d_1$  can be calculated using Eq. 3.9-3.11.

Table 4: Parameters corresponding  $\chi^2 = 0.083$  for normal mass ordering.

$a'$	$e'$	$f'$	$b'_2$	$c'_2$	$d'_2$	$\chi^2$
-0.036	-0.050	0.003	-0.052	-0.059	-0.122	0.083

Finally, given the rescaled data set for that  $\chi_{min}^2$ ,  $M_1$  is varied widely to have  $Y_B$  in the observed range. For each value of  $M_1$ , a set of values of the unprimed parameters

$\{a, e, f, b_1, c_1, d_1, b_2, c_2, d_2\}$  is generated. Final  $Y_B$  is then calculated for each values of  $M_1$  and the corresponding unprimed set. An experimentally appealing conclusion of this scheme is that, given the observed range of  $Y_B$ , the octant of  $\theta_{23}$  is determined. From the plot on the right panel of Fig 6, one can see that the value of  $k$  is always greater that 1. Thus on account of the relation  $\tan \theta_{23} = k^{-1}$ ,  $\theta_{23}$  always lie below  $45^\circ$ . Here the red narrow strip in the said plot represents the observed range of  $Y_B$ .

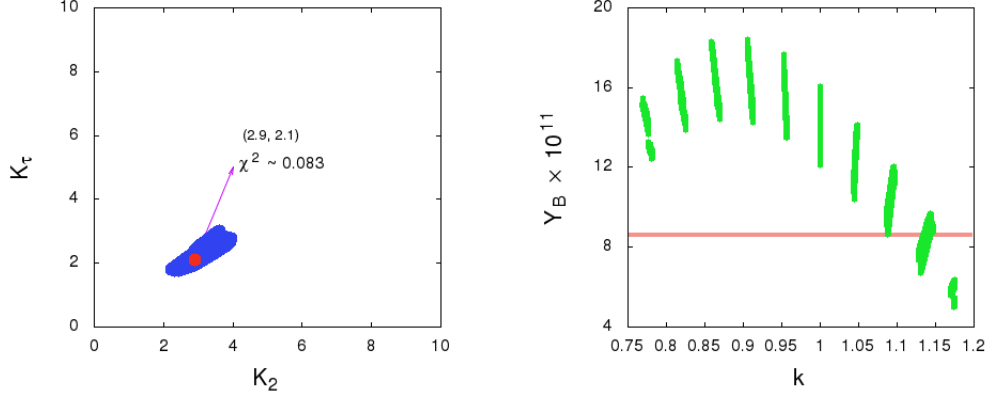


Figure 6: The plot on the left hand side shows the range of the wash-out parameters. The red dot corresponds to the minimum value of  $\chi^2$  for which a set of rescaled parameter has been taken to compute  $Y_B$ . The plot on the right hand side shows a variation of  $Y_B$  vs  $k$ . The red band in the same plot indicates the observed range of  $Y_B$ .

A careful surveillance of the plot in Fig 7 leads to the conclusion that we can obtain an upper and a lower bound on  $M_1$  due to the observed constraint on  $Y_B$ . In order to appreciate

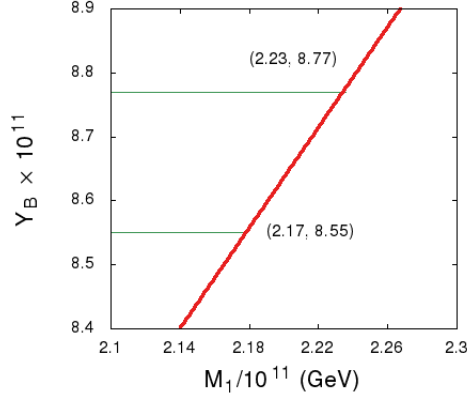


Figure 7: A plot of the final  $Y_B$  for different values of  $M_1$  for a normal light neutrino mass ordering.

this fact more clearly, two straight lines have been drawn parallel to the abscissa in the mentioned plot: one at  $Y_B = 8.55 \times 10^{-11}$  and the other at  $Y_B = 8.77 \times 10^{-11}$ . The values of  $M_1$ ,

where the straight lines meet the  $Y_B$  vs  $M_1$  curve, yield the allowed lower and upper bounds on  $M_1$ , namely  $(M_1)_{lower} = 2.17 \times 10^{11}$  GeV and  $(M_1)_{upper} = 2.23 \times 10^{11}$  GeV.

**$M_1 > 10^{12}$  GeV:** It has been shown that  $Y_B = 0$  here for our model.

### $Y_B$ for inverted mass ordering of light neutrinos:

Proceeding exactly in the same manner as for the normal mass ordering, a final discussion for each regime goes as follows.

**$M_1 < 10^9$  GeV:** Similar to the normal ordering, the  $|\varepsilon_1^{\mu,\tau}|$  can have values at most the order of  $10^{-8}$  which is not sufficient to let  $Y_B$  come within its observed range.

**$10^9$  GeV  $< M_1 < 10^{12}$  GeV:** Unlike the previous case the ranges of the the wash-out parameters (cf. Fig 8) favors a strong wash-out scenario. Thus the efficiency factor in Eq.(4.14) can be written for this strong wash-out scenario [22] as

$$\eta(\tilde{m}_\alpha) = \left[ \left( \frac{0.55 \times 10^{-3}}{\tilde{m}_\alpha} \right)^{1.16} \right]. \quad (5.10)$$

For  $\chi_{min}^2 = 0.261$ , a set of rescaled parameters is obtained (cf Table 5). Then similar to the previous case varying  $M_1$  in a wide range a lower and upper bound on  $M_1$ , namely  $(M_1)_{lower} = 5.52 \times 10^{11}$  GeV and  $(M_1)_{upper} = 5.66 \times 10^{11}$  GeV is obtained for the observed range of  $Y_B$ . A plot of  $Y_B$  vs  $M_1$  is shown in the right panel of Fig. 8.

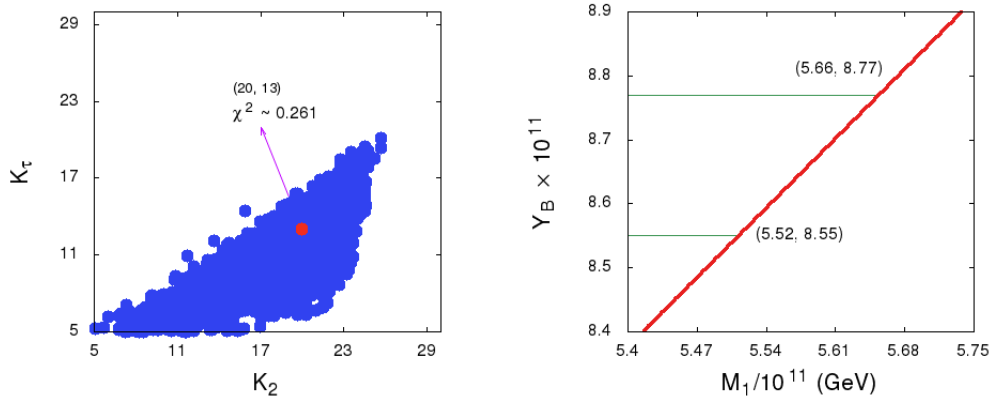


Figure 8: The plot on the left hand side shows the range of the wash-out parameters. The red dot corresponds to the minimum value of  $\chi^2$  for which a set of rescaled parameter has been taken to compute  $Y_B$ . The plot on the right hand side shows final  $Y_B$  for different values of  $M_1$  for the inverted light neutrino mass ordering.

Table 5: Parameters corresponding  $\chi^2 = 0.261$  for inverted hierarchy

$a'$	$e'$	$f'$	$b'_2$	$c'_2$	$d'_2$	$\chi^2$
-0.043	-0.065	0.116	0.130	-0.019	0.039	0.261

$M_1 > 10^{12}$  GeV: Once again,  $Y_B = 0$  here for the present model.

**Case-II:  $Y_B$  for normal mass ordering of light neutrinos:**

The analysis has been done exactly in the same way as was in the previous case. A systematic presentation of the obtained results is the following.

$M_1 < 10^9$  GeV: Again,  $Y_B$  in the observed range cannot be generated due to the small value of  $|\varepsilon_1^{\mu,\tau}|$ .

$10^9$  GeV  $< M_1 < 10^{12}$  GeV: Similar to the previous normal hierarchical case, the wash-out parameters here also suggest a mild wash-out scenario (cf. Fig. 9).

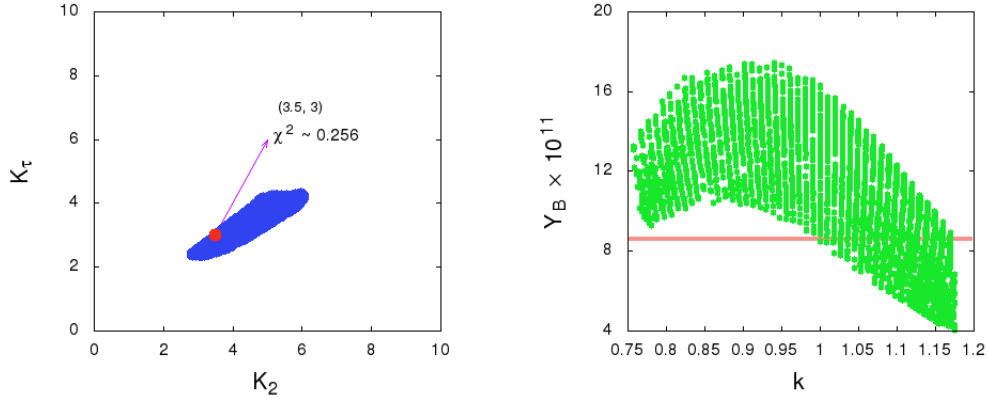


Figure 9: The plot on the left hand side shows the range of the wash-out parameters. The red dot corresponds to the minimum value of  $\chi^2$  for which a set of rescaled parameter has been taken to compute  $Y_B$ . The plot on the right hand side shows a variation of  $Y_B$  vs  $k$ . The red band in the same plot indicates the observed range of  $Y_B$ .

For  $\chi_{min}^2 = 0.256$ , a set of rescale parameter has been found and then varying  $M_1$  in a wide range, a lower and a upper bound on  $M_1$  are obtained as shown in the Fig. 10. In this case also for  $Y_B$  to be in the observed range, the predicted values of  $\theta_{23}$  prefer to lie below the  $45^\circ$ .

Table 6: Parameters corresponding  $\chi^2 = 0.256$  for normal mass ordering.

$a'$	$e'$	$f'$	$b'_2$	$c'_2$	$d'_2$	$\chi^2$
-0.042	-0.046	-0.005	-0.065	-0.056	-0.128	0.256

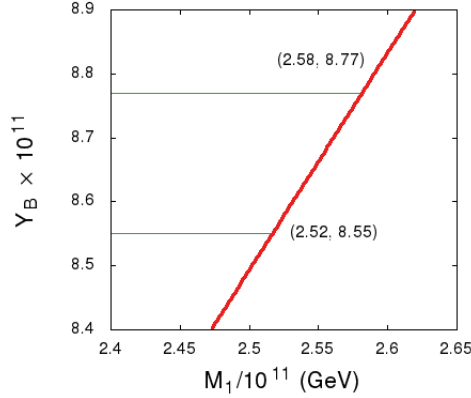


Figure 10: A plot of the final  $Y_B$  for different values of  $M_1$  for the normal light neutrino mass ordering.

**$M_1 > 10^{12}$  GeV:** It has been shown that  $Y_B = 0$  here for our model.

**$Y_B$  for inverted mass ordering of light neutrinos:**

Proceeding exactly in the same manner as for the normal mass ordering, a final discussion for each regime goes as follows.

**$M_1 < 10^9$  GeV:** Similar to the normal ordering, the  $|\varepsilon_1^{\mu,\tau}|$  can have values at most the order of  $10^{-8}$  which is not sufficient to let  $Y_B$  come within its observed range.

**$10^9$  GeV  $< M_1 < 10^{12}$  GeV:** Unlike the previous case the ranges of the the wash-out parameters (cf. Fig 11) favors a strong wash-out scenario. For  $\chi_{min}^2 = 0.041$  a set of rescaled parameters is obtained (cf Table 7). Then similar to the previous case varying  $M_1$  in a wide range a lower and upper bound on  $M_1$ , namely  $(M_1)_{lower} = 5.27 \times 10^{11}$  GeV and  $(M_1)_{upper} = 5.40 \times 10^{11}$  GeV is obtained for the observed range of  $Y_B$ . A plot of  $Y_B$  vs  $M_1$  is shown in the right panel of Fig. 11.

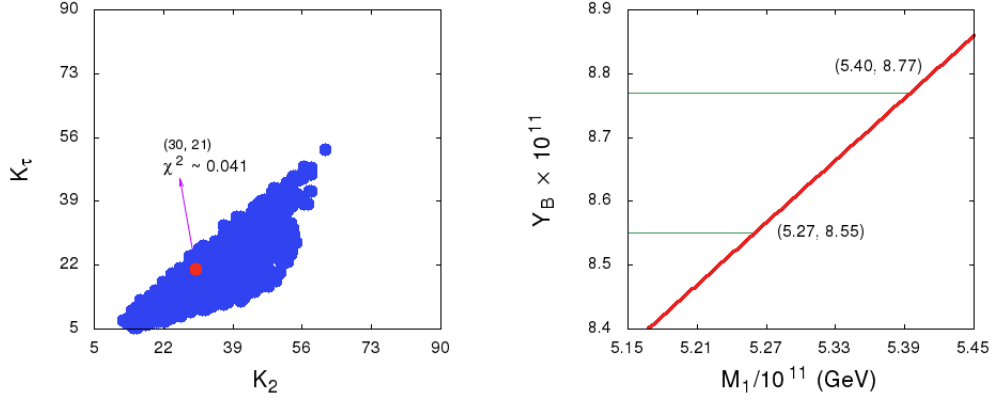


Figure 11: The plot on the left hand side shows the range of the wash-out parameters. The red dot corresponds to the minimum value of  $\chi^2$  for which a set of rescaled parameter has been taken to compute  $Y_B$ . The plot on the right hand side shows final  $Y_B$  for different values of  $M_1$  for the inverted light neutrino mass ordering.

Table 7: Parameters corresponding  $\chi^2 = 0.041$  for inverted hierarchy

$a'$	$e'$	$f'$	$b'_2$	$c'_2$	$d'_2$	$\chi^2$
-0.123	-0.084	0.123	0.104	-0.052	-0.096	0.041

$M_1 > 10^{12}$  GeV: Once again,  $Y_B = 0$  here for the present model.

A compact presentation of the final conclusions regarding  $Y_B$  from the numerical analysis is given in Table 8. Before concluding this section we want to stress the following point. This is a model where the imaginary part of  $m_D^{MS}$  of Eq. 3.8 plays a crucial role. Absence of the latter leads to a vanishing  $\theta_{13}$  thus undetermined value of  $\delta$  and most importantly a vanishing value of  $\varepsilon_i^\alpha$ . Thus the model addresses a common origin of  $\theta_{13}$ , CP violation and leptogenesis. However, although the parameters in the imaginary part of  $m_D^{MS}$  are correlated with  $Y_B$ , we found no such significant correlation of the latter with the parameters  $a$ ,  $e$  and  $f$ . The value  $Y_B$  of randomly fluctuates from a negative to a positive value.

Table 8: Final statements on  $Y_B$  for different mass regimes.

Case-I			
Type	$M_1 < 10^9$ GeV	$10^9$ GeV $< M_1 < 10^{12}$ GeV	$M_1 > 10^{12}$ GeV
Normal Ordering	Ruled out since $Y_B$ is below the observed range for any $\chi^2$ .	$Y_B$ within the observed range for $\chi_{min}^2 = 0.083$ .	Ruled out since $Y_B = 0$ .
Inverted Ordering	Ruled out since $Y_B$ is below the observed range for any $\chi^2$ .	$Y_B$ within the observed range for $\chi_{min}^2 = 0.261$ .	Ruled out since $Y_B = 0$ .
Case-II			
Type	$M_1 < 10^9$ GeV	$10^9$ GeV $< M_1 < 10^{12}$ GeV	$M_1 > 10^{12}$ GeV
Normal Ordering	Ruled out since $Y_B$ is below the observed range for any $\chi^2$ .	$Y_B$ within the observed range for $\chi_{min}^2 = 0.256$ .	Ruled out since $Y_B = 0$ .
Inverted Ordering	Ruled out since $Y_B$ is below the observed range for any $\chi^2$ .	$Y_B$ within the observed range for $\chi_{min}^2 = 0.041$ .	Ruled out since $Y_B = 0$ .

## 6 Effect of $N_{2,3}$ on $Y_B$

In our analysis, the effect of the two heavier neutrinos ( $N_2, N_3$ ) on the produced final baryon asymmetry has been neglected with the assumption that the asymmetries produced by the decays of both of them get washed out [20]. In this section we present an ephemeral discussion on the sensitivity of the heavier neutrino to final  $Y_B$ . There are two ways that such a sensitivity might arise as elaborated below.

### Indirect effect of $N_{2,3}$ :

Though the neutrino oscillation data are fitted with the rescaled (primed) parameters, cf (5.1), for computing the quantities related to leptogenesis, e.g.,  $\varepsilon_1^\alpha$ , we need to evaluate the unprimed ones, i.e. the Dirac mass matrix elements. It is interesting to see whether the final baryon asymmetry is affected by the chosen hierarchies of the RH neutrinos. We find that the final  $Y_B$  is not much sensitive to  $M_{2,3}$ . One can appreciate this statement by simplifying the CP asymmetry parameters of (4.2) to

$$\varepsilon_1^\alpha = -\frac{3}{8\pi v^2 h_{11}} \sum_{j=2,3} \frac{M_1}{M_j} \text{Im}[h_{1j}(m_D)_{1\alpha}(m_D^*)_{j\alpha}] - \frac{1}{4\pi v^2 h_{11}} \sum_{j=2,3} \frac{M_1^2}{M_j^2} \text{Im}[h_{j1}(m_D)_{1\alpha}(m_D^*)_{j\alpha}] \quad (6.1)$$

after approximating  $g(x_{1j})$  of Eqs. (4.3) to  $g(x_{1j}) = -\frac{3}{2\sqrt{x_{1j}}}$  for  $x_{1j} \gg 1$ . The last term of Eq. (6.1) is suppressed because it is of second order in  $x_{1j}^{-1}$ . Having two parts for  $j = 2, 3$ ,  $j = 3$



term of the first term of Eq. 6.1 has a negligible effect on  $\varepsilon_1^\alpha$  since  $M_3$  is much larger than  $M_1$  and  $f, d_1$  and  $d_2$  have values of the order of the other Dirac components. Now for  $j = 2$ ,  $\varepsilon_1^\alpha$  is simplified as

$$\varepsilon_1^\mu = -\frac{3M_1}{8\pi v^2 h_{11}}[(ae' + b_1c'_1 + b_2c'_2)(b_2c'_1 + b_1c'_2)] = -\varepsilon_1^\tau \quad (6.2)$$

with  $\varepsilon_1^e = 0$  as already shown in Sec. 4. Since the primed parameters are fixed by the oscillation data,  $\varepsilon_1^{\mu,\tau}$  are practically insensitive to the value of  $M_2$ . However, for the numerical computation of the final baryon asymmetry, we take into account each term in (6.1) with two different mass hierarchical schemes for the heavy neutrinos, e.g,  $M_{i+1}/M_i = 10^2$  and  $M_{i+1}/M_i = 10^4$  where  $i$  can take the values 1, 2. Note that in the previous section we have already computed  $Y_B$  for  $M_{i+1}/M_i = 10^3$ . The outcome of the numerical analysis is that though the chosen mass ratios of the RH neutrinos are altered, changes in the lower and upper bounds on  $M_1$  are not significant for the observed range of  $Y_B$ . For convenience, For each case and light neutrino mass ordering, the variation of  $Y_B$  with  $M_1$  for different mass ratios has been presented in Table 9.

Table 9: Lower and upper bounds on  $M_1$  for different mass ratios of the RH neutrinos ( $i = 1, 2$ ).

Case-I: Normal light neutrino ordering			
Hierarchies $\rightarrow$	$M_{i+1}/M_i = 10^2$	$M_{i+1}/M_i = 10^3$	$M_{i+1}/M_i = 10^4$
Upper bound (GeV)	$2.21 \times 10^{11}$	$2.23 \times 10^{11}$	$2.25 \times 10^{11}$
Lower bound (GeV)	$2.16 \times 10^{11}$	$2.17 \times 10^{11}$	$2.18 \times 10^{11}$
Case-I: Inverted light neutrino ordering			
Hierarchies $\rightarrow$	$M_{i+1}/M_i = 10^2$	$M_{i+1}/M_i = 10^3$	$M_{i+1}/M_i = 10^4$
Upper bound (GeV)	$5.64 \times 10^{11}$	$5.66 \times 10^{11}$	$5.67 \times 10^{11}$
Lower bound (GeV)	$5.51 \times 10^{11}$	$5.52 \times 10^{11}$	$5.54 \times 10^{11}$
Case-II: Normal light neutrino ordering			
Hierarchies $\rightarrow$	$M_{i+1}/M_i = 10^2$	$M_{i+1}/M_i = 10^3$	$M_{i+1}/M_i = 10^4$
Upper bound (GeV)	$2.57 \times 10^{11}$	$2.58 \times 10^{11}$	$2.59 \times 10^{11}$
Lower bound (GeV)	$2.50 \times 10^{11}$	$2.52 \times 10^{11}$	$2.54 \times 10^{11}$
Case-II: Inverted light neutrino ordering			
Hierarchies $\rightarrow$	$M_{i+1}/M_i = 10^2$	$M_{i+1}/M_i = 10^3$	$M_{i+1}/M_i = 10^4$
Upper bound (GeV)	$5.38 \times 10^{11}$	$5.40 \times 10^{11}$	$5.42 \times 10^{11}$
Lower bound (GeV)	$5.25 \times 10^{11}$	$5.27 \times 10^{11}$	$5.28 \times 10^{11}$

### Direct effect of $N_2$ :

For simplicity, here we consider only the effect of  $N_2$ . It is shown in Ref. [21] that, due to a decoherence effect, a finite amount of lepton asymmetry generated by  $N_2$  decays get protected

against  $N_1$ -washout thus survive down to the electroweak scale and contribute to the final

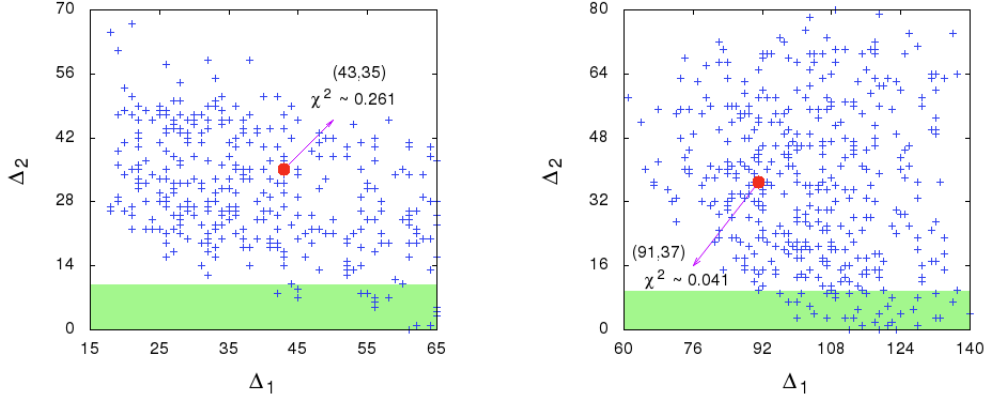


Figure 12: Plots of the wash-out parameters  $\Delta_1$  and  $\Delta_2$  for inverted light neutrino mass ordering for both the cases. The red dot corresponds to the corresponding  $\chi^2_{min}$  for which we calculate the final baryon asymmetry.

baryon asymmetry. For this procedure to happen, two wash-out parameters  $\Delta_1 = \frac{h_{11}}{M_1 m^*}$  and  $\Delta_2 = \frac{h_{22}}{M_2 m^*}$  must satisfy the condition  $\Delta_1 \gg 1$  and  $\Delta_2 \not\gg 1$  with  $m^* = 1.66\sqrt{g^*}\pi v^2/M_{Pl} \approx 10^{-3}$  eV. Here  $\Delta_1 \gg 1$  indicates that faster  $N_1$  interactions destroy coherence among the states produced by  $N_2$ , thus a part of the lepton asymmetry produced by  $N_2$  survives orthogonal to  $N_1$ -states and gets protected against  $N_1$ -washout. On the other hand, a mild wash-out of the lepton asymmetry produced by  $N_2$  due to  $N_2$ -related interactions is represented by  $\Delta_2 \not\gg 1$  condition. For this mild wash-out scenario, a sizable  $N_2$ -generated lepton asymmetry survives during the  $N_1$ -leptogenesis phase. It has been found that for each of the discussed cases, for a normal light neutrino mass ordering, both the wash-out parameters  $\Delta_{1,2} < 10$ . Thus faster  $N_1$  interaction do not take place and condition for  $N_2$  leptogenesis is violated. On the other hand for inverted light neutrino mass orderings, the allowed parametric region prefers large values of  $\Delta_2$  in excess of 10 except at the bottom (green band). Thus the  $\Delta_2 \not\gg 1$  condition is violated in most of the region. Moreover the  $\chi^2_{min}$  values, for which we calculate final  $Y_B$  strongly violates  $\Delta_2 \not\gg 1$  condition. Few allowed points with  $\Delta_2 < 10$  correspond to values of  $\chi^2$  above 0.8 which is much higher than  $\chi^2_{min}$  for which we obtain  $Y_B$  in the observed range. Therefore, for our calculation, any direct effect of  $N_2$  is not significant.

## 7 Summary and conclusion

We present the Strong Scaling Ansatz (SSA) as a residual  $\mathbb{Z}_2 \times \mathbb{Z}_2$  symmetry. Since SSA predict a vanishing  $\theta_{13}$ —thus no Dirac CP violation, we modify SSA with an complex extension of the residual  $\mathbb{Z}_2 \times \mathbb{Z}_2$  by invoking a nonstandard CP transformation and address the new symmetry as a generalized  $\mathbb{Z}_2 \times \mathbb{Z}_2$  symmetry. Depending upon the implementation of the symmetry,

there are several cases that have been explored in this model. For each of the cases, beside the absorbing predictions of maximal Dirac CP violation ( $\delta = \pm\pi/2$ ) and CP conserving values for the Majorana phases ( $\alpha, \beta = 0, \pi$ ), constrained ranges for the  $\beta\beta 0\nu$  decay parameter  $|M_{ee}|$  and the light neutrino masses are also found. In this extended SSA, both the neutrino mass orderings are found to be allowed with upper bounds on  $\sum_i m_i$  that are much lower than the present value 0.23 eV.

We further discuss the generalized  $\mathbb{Z}_2 \times \mathbb{Z}_2$  within the framework of type-I seesaw mechanism. Baryogenesis via leptogenesis scenario has been explored qualitatively as well as quantitatively. Typical structure of the Dirac mass matrix  $m_D$  leads to a common origin of  $\theta_{13}$ , leptonic CP violation and nonzero CP asymmetry parameter  $\varepsilon_i^\alpha$ . Here we focus the  $N_1$ -leptogenesis scenario as the primary one, with a discussion on  $N_{2,3}$ -leptogenesis which is not so sensitive to our final results. For each of the cases and irrespective of the light neutrino mass ordering, only  $\tau$ -flavored leptogenesis scenario ( $10^9 \text{ GeV} < T \sim M_1 < 10^{12} \text{ GeV}$ ) is found to be feasible one to generate  $Y_B$  in the observed range with the other regimes  $T \sim M_1 > 10^{12}$  and  $T \sim M_1 < 10^9 \text{ GeV}$  being ruled out analytically as well as numerically. We also found an upper and a lower bound on the lightest ( $M_1$ ) of the heavy neutrino masses for each case. Although both the light neutrino mass orderings are allowed, the normal mass ordering comes up with an interesting prediction. For both the allowed cases and for a normal mass ordering, it has been found that for  $Y_B$  to be in the observed range,  $\theta_{23}$  must be less than its maximal value.

As a final note, the predictions of this model—thus the viability of modification to SSA with a generalized  $\mathbb{Z}_2 \times \mathbb{Z}_2$  symmetry, would be tested in the ongoing experiments such as GERDA-II [29], T2K [31], NO $\nu$ A [32] etc. shortly.

## Acknowledgment

The work of the authors are supported by the the Department of Atomic Energy (DAE), Government of India. The authors would like to thank Prof. Probir Roy for discussion about residual symmetry. R. Samanta would like to thank Prof. Walter Grimus for a valuable discussion on CP transformation during a visit at the University of Vienna.

## References

- [1] C.S Lam, Phys. Lett B **656**, 193 (2007); Phys. Rev. Lett. **101**, 121602 (2008); Phys. Rev. D **78**, 073015 (2008).
- [2] D. A. Dicus, S. F. Ge and W. W. Repko, Phys. Rev. D **83**, 093007 (2011), Phys. Lett. B **702**, 220 (2011), Phys. Rev. Lett. **108**, 041801 (2012).

- [3] F. Feruglio, C. Hagedorn and R. Ziegler, JHEP **1307**, 027 (2013), R. N. Mohapatra and C. C. Nishi, JHEP **1508**, 092 (2015).
- [4] P. Byakti and P. B. Pal, [arXiv:1601.08063](https://arxiv.org/abs/1601.08063) [hep-ph].
- [5] W. Grimus and L. Lavoura, Acta Phys. Polon. B **34**, 5393 (2003); Phys. Lett. B **579**, 113 (2004); Fortsch. der Phys. **61**, 535 (2013).
- [6] S. Gupta, A. S. Joshipura and K. M. Patel, Phys. Rev. D **85**, 031903 (2012)
- [7] L. Lavoura, Phys. Rev. D **62**, 093011 (2000). R. N. Mohapatra and W. Rodejohann, Phys. Lett. B **644**, 59 (2007).
- [8] A. S. Joshipura and W. Rodejohann, Phys. Lett. B **678**, 276 (2009). A. Ghosal and R. Samanta, JHEP **1505**, 077 (2015), R. Samanta, M. Chakraborty and A. Ghosal, Nucl. Phys. B **904**, 86 (2016).
- [9] F. P. An *et al.* [Daya Bay Collaboration], Phys. Rev. Lett. **115**, 111802 (2015).
- [10] P. Chen, G. J. Ding, F. Gonzalez-Canales and J. W. F. Valle, Phys. Lett. B **753**, 644 (2016).
- [11] P. A. R. Ade *et al.* [Planck Collaboration], Astron. Astrophys. **594**, A13 (2016).
- [12] K.A Olive et al [Particle Data Group] Chinese Physics C38, 090001 (2014).
- [13] G. Ecker, W. Grimus, H. Neufeld, J.Phys. A20, L807 (1987); Int.J.Mod.Phys. A3, 603 (1988). W. Grimus and M. N. Rebelo, Phys. Rept. 281, 239 (1997). G. J. Ding, S. F. King and A. J. Stuart, JHEP **1312**, 006 (2013). C. Hagedorn, A. Meroni and E. Molinaro, Nucl. Phys. B **891**, 499 (2015). P. Chen, C. Y. Yao and G. J. Ding, Phys. Rev. D **92**, no. 7, 073002 (2015).
- [14] R. Samanta, P. Roy and A. Ghosal, Eur. Phys. J. C **76**, no. 12, 662 (2016), R. Samanta, P. Roy and A. Ghosal, Acta Phys. Polon. Supp. **9**, 807 (2016).
- [15] P. Chen, G. J. Ding and S. F. King, JHEP **1603**, 206 (2016). R. Samanta, M. Chakraborty, P. Roy and A. Ghosal, JCAP **1703**, no. 03, 025 (2017).
- [16] M. Fukugita and T. Yanagida, Phys. Lett. B **174**, 45 (1986).
- [17] J. M. Cline, [hep-ph/0609145](https://arxiv.org/abs/hep-ph/0609145). W. Buchmuller, P. Di Bari and M. Plumacher, Annals Phys. **315**, 305 (2005) S. Davidson, E. Nardi and Y. Nir, Phys. Rept. **466**, 105 (2008). E. Bertuzzo, P. Di Bari, F. Feruglio and E. Nardi, JHEP **0911**, 036 (2009).
- [18] G.'t Hooft, Phys. Rev. D **14**, 3442 (1976).

- [19] A. Pilaftsis and T.E.J. Underwood, Nucl. Phys. **B692** (2004) 392. B. Adhikary, M. Chakraborty and A. Ghosal, Phys. Rev. D **93**, 113001 (2016).
- [20] W. Buchmuller, P. Di Bari and M. Plumacher, Nucl. Phys. B **665**, 445 (2003).
- [21] G. Engelhard, Y. Grossman, E. Nardi and Y. Nir, Phys. Rev. Lett. **99**, 081802 (2007).
- [22] A. Abada, S. Davidson, A. Ibarra, F.-X Josse-Michaux, M. Losada and A. Riotto, JHEP **0609** (2006) 010.
- [23] M. C. Gonzalez-Garcia, M. Maltoni and T. Schwetz, Nucl. Phys. B **908**, 199 (2016)
- [24] C.S Lam, Phys. Lett B **656**, 193 (2007); Phys. Rev. Lett. **101**, 121602 (2008); Phys. Rev. D **78**, 073015 (2008).
- [25] W. Rodejohann, Int. J. Mod. Phys. E **20**, 1833 (2011). P. S. Bhupal Dev, S. Goswami, M. Mitra and W. Rodejohann, Phys. Rev. D **88**, 091301 (2013).
- [26] M. Auger *et al.* [EXO-200 Collaboration], Phys. Rev. Lett. **109**, 032505 (2012)
- [27] K. Asakura *et al.* [KamLAND-Zen Collaboration], Nucl. Phys. A **946**, 171 (2016)
- [28] M. Agostini *et al.* [GERDA Collaboration], Phys. Rev. Lett. **111**, no. 12, 122503 (2013)
- [29] B. Majorovits [GERDA Collaboration], AIP Conf. Proc. **1672**, 110003 (2015)
- [30] N. Abgrall *et al.* [Majorana Collaboration], Adv. High Energy Phys. **2014**, 365432 (2014)
- [31] K. Abe *et al.* [T2K Collaboration], Phys. Rev. D **91**, no. 7, 072010 (2015)
- [32] J. Bian [NOvA Collaboration], [arXiv:1510.05708](https://arxiv.org/abs/1510.05708) [hep-ex].